

Supplementary Information

A multifunctional microporous anionic metal–organic framework for column-chromatographic dye separation and selective detection and adsorption of Cr³⁺

Shu-Ran Zhang,^a Jing Li,^a Dong-Ying Du,^{*a} Jun-Sheng Qin,^a Shun-Li Li,^b Wen-Wen He,^a Zhong-Min Su^{*a} and Ya-Qian Lan^{*a,b}

^a Institute of Functional Material Chemistry, Faculty of Chemistry, Northeast Normal University, Changchun 130024, Jilin, People's Republic of China. E-mail: zmsu@nenu.edu.cn

^b Jiangsu Key Laboratory of Biofunctional Materials, School of Chemistry and Materials Science, Nanjing Normal University, Nanjing 210023, Jiangsu, People's Republic of China. E-mail: yqlan@njnu.edu.cn

Table S1 Crystal data and structure refinements for **NENU-505**.

Identification code	NENU-505
Formula	C ₁₄ H ₂₆ N _{3.5} O _{9.5} Zn
Formula weight	460.18
Crystal system	Monoclinic
Space group	C2/c
<i>a</i> (Å)	27.7680(11)
<i>b</i> (Å)	7.9000(6)
<i>c</i> (Å)	18.2980(14)
α (°)	90.00
β (°)	108.3290(15)
γ (°)	90.00
<i>V</i> (Å ³)	3810.3(4)
<i>Z</i>	4
<i>D</i> _{calcd} ·[g cm ⁻³]	1.114
<i>F</i> (000)	1300
Reflections collected	13597
<i>R</i> (int)	0.0330
Goodness-of-fit on <i>F</i> ²	0.834
<i>R</i> ₁ ^a [<i>I</i> >2σ (<i>I</i>)]	0.0479
<i>wR</i> ₂ ^b	0.1464

$$^a R_1 = \sum |F_o| - |F_c| / \sum |F_o|. \quad ^b wR_2 = \left| \sum w(|F_o|^2 - |F_c|^2) \right| / \left| \sum w(F_o^2)^2 \right|^{1/2}.$$

Table S2 The selected bond lengths [Å] and angles [deg] for **NENU-505**.

Bond length [Å]	Bond angle [deg]		
Zn(1)-O(3)	1.910(2)	O(3)-Zn(1)-O(5)	113.55(11)
Zn(1)-O(5)	1.930(2)	O(3)-Zn(1)-O(2)#1	114.98(10)
Zn(1)-O(2)#1	1.9476(19)	O(5)-Zn(1)-O(2)#1	112.06(12)
Zn(1)-O(1)#2	1.9615(18)	O(3)-Zn(1)-O(1)#2	94.48(9)
		O(5)-Zn(1)-O(1)#2	109.41(12)
		O(2)#1-Zn(1)-O(1)#2	110.97(10)

Symmetry transformations used to generate equivalent atoms: #1 *x*, -*y*, *z*+1/2; #2 -*x*, -*y*, -*z*.

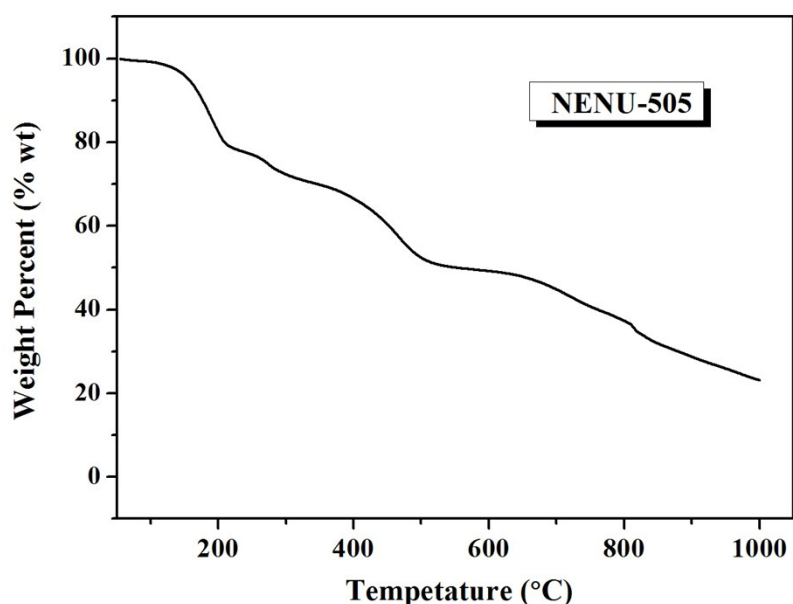


Fig. S1 The TGA curve of **NENU-505** was measured under N_2 atmosphere from 50 °C to 1000 °C at the heating rate of 10 °C·min⁻¹.

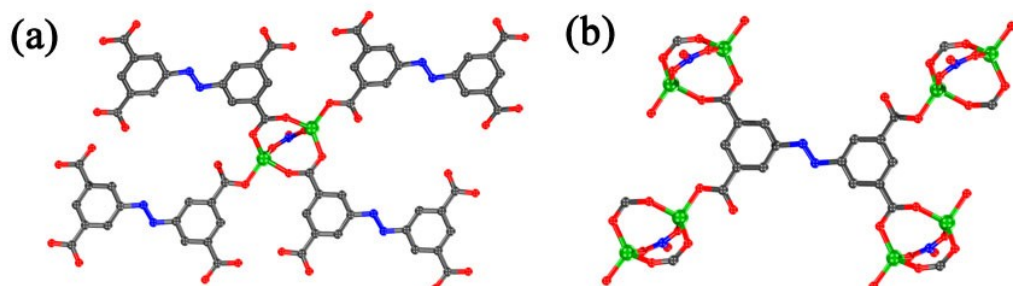


Fig. S2 Coordination environments of (a) binuclear $[\text{Zn}_2(\text{CO}_2)_4(\text{NO}_3)]$ cluster and (b) the H₄ABTC ligand in **NENU-505**, respectively.

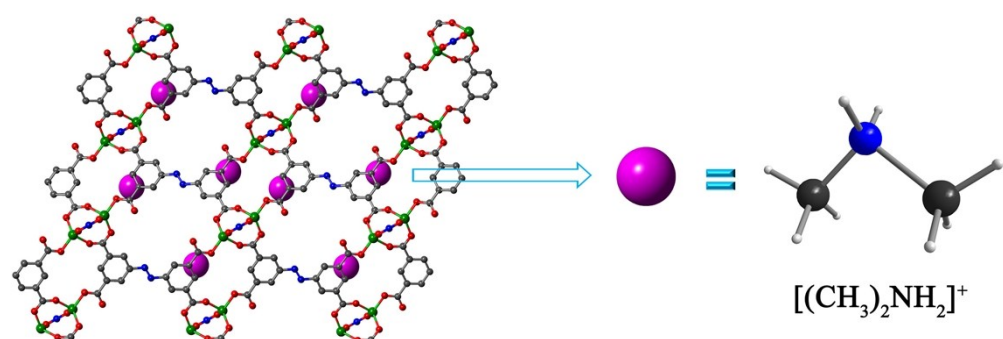


Fig. S3 The schematic representation of $[(\text{CH}_3)_2\text{NH}_2]^+$ ions located in the 3D framework of **NENU-505** along the *b* axis.

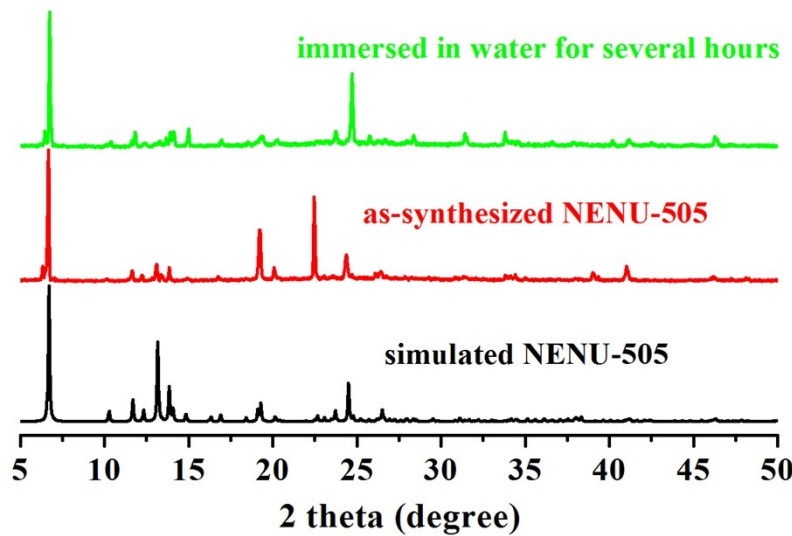


Fig. S4 XRPD patterns of simulated NENU-505 (black), as-synthesized NENU-505 (red) and immersed in water for a few hours (green).

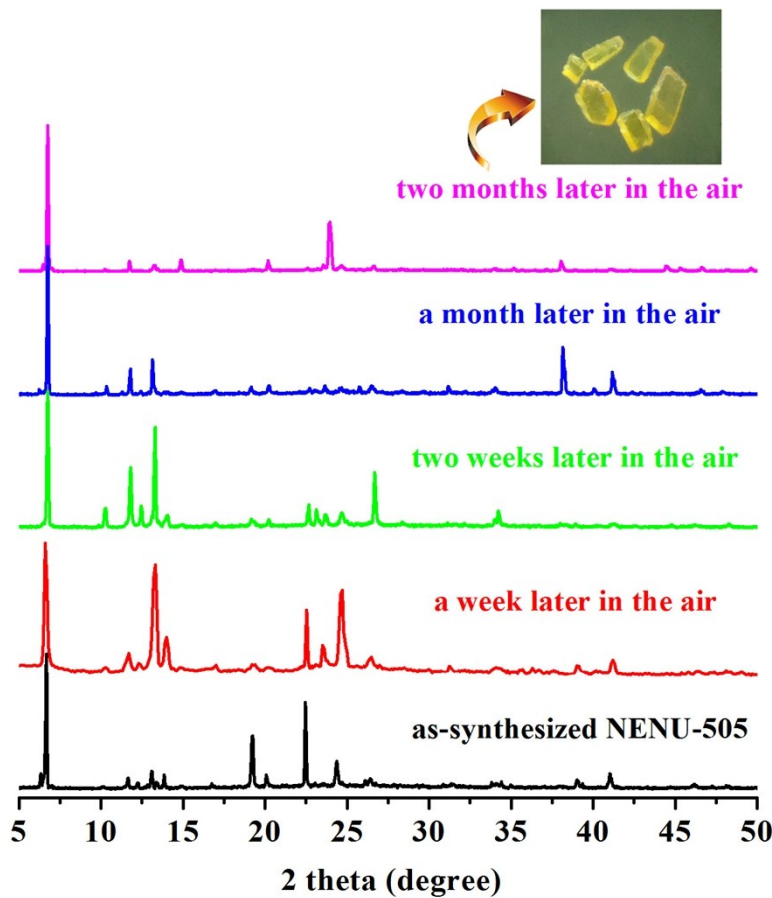


Fig. S5 XRPD patterns of as-synthesized NENU-505 (black) and NENU-505 samples exposed in the air after a week (red), two weeks (green), a month (blue) and two months (pink), respectively. Inset: the optical image of NENU-505 exposed after two months in the air.

Table S3 Comparison of MB adsorption capacity in various adsorbents.

Materials	Adsorption capacity (mg g ⁻¹)	Ref.
Graphene oxide	397	1
ErCu-POM (Er-3)	391.3	2
PW ₁₁ V@MIL-101	371	3
Cd-MOF (2)	317.9	4
Activated carbon	135	5
Zn-DDQ	135	6
Cd-MOF (1)	105	4
Cu-DDQ	90	6
Pb-DDQ	86	6
NENU-505	33.5	This work
Cd-MOF (3)	30	4
MOF@graphite oxide	18	7
446-MOF	17	8
Zn-MOF	0.75	9

Table S4 The adsorption capacity of **NENU-505** at room temperature for every dye.

Dye composition	Adsorption capacity for MB (mg g ⁻¹)	Adsorption capacity for BR 2 (mg g ⁻¹)	Adsorption capacity for BG 1 (mg g ⁻¹)
Single component dye (MB)	33.5	_UD ^[a]	_UD ^[a]
Single component dye (BR 2)	_UD ^[a]	4.5	_UD ^[a]
Single component dye (BG 1)	_UD ^[a]	_UD ^[a]	17.6
Mixture dye (MB and BR 1)	33.3	_UD ^[a]	_UD ^[a]
Mixture dye (MB and MO)	33.4	_UD ^[a]	_UD ^[a]
Mixture dye (BG 1 and BR 1)	_UD ^[a]	_UD ^[a]	17.3

[a] UD: undetected

Table S5 The ICP percentage of Cr³⁺ encapsulated by **NENU-505** in multi-element solutions.

Multi-element solution	The ICP percentage of Cr ³⁺ (%)
1: Fe ²⁺ , Cu ²⁺ and Cr ³⁺	4.056
2: Cu ²⁺ , Ni ²⁺ and Cr ³⁺	4.009
3: Cu ²⁺ , Co ²⁺ and Cr ³⁺	3.858
4: Ni ²⁺ , Co ²⁺ and Cr ³⁺	4.069

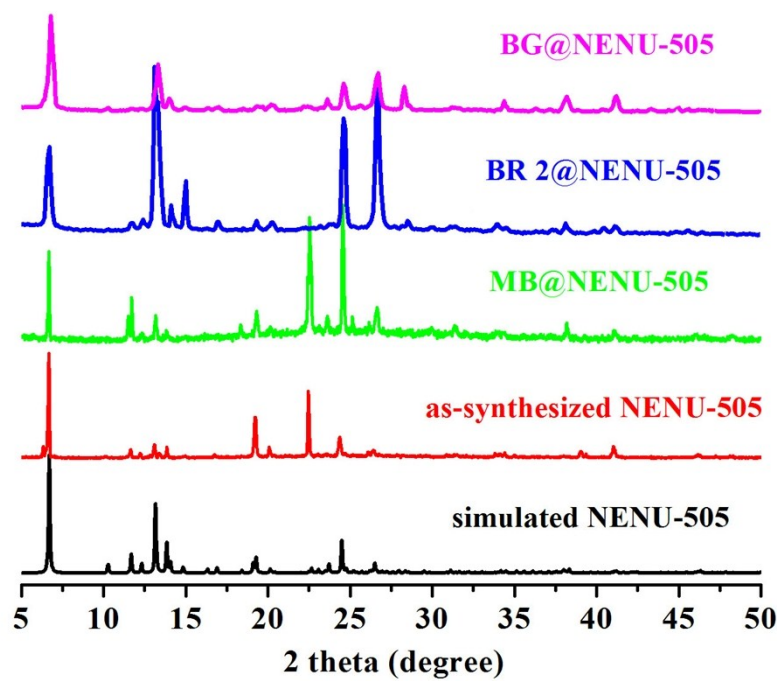


Fig. S6 XRPD patterns of simulated NENU-505 (black), as-synthesized NENU-505 (red) and after the absorption of MB (green), BR 2 (blue) and BG (pink), respectively.

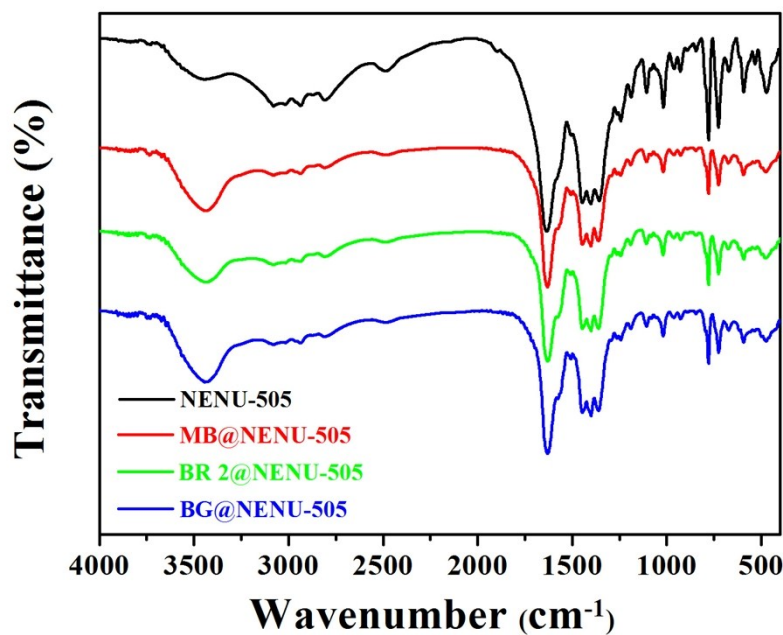


Fig. S7 IR spectra of NENU-505, MB@NENU-505, BR 2@NENU-505, and BG@NENU-505.

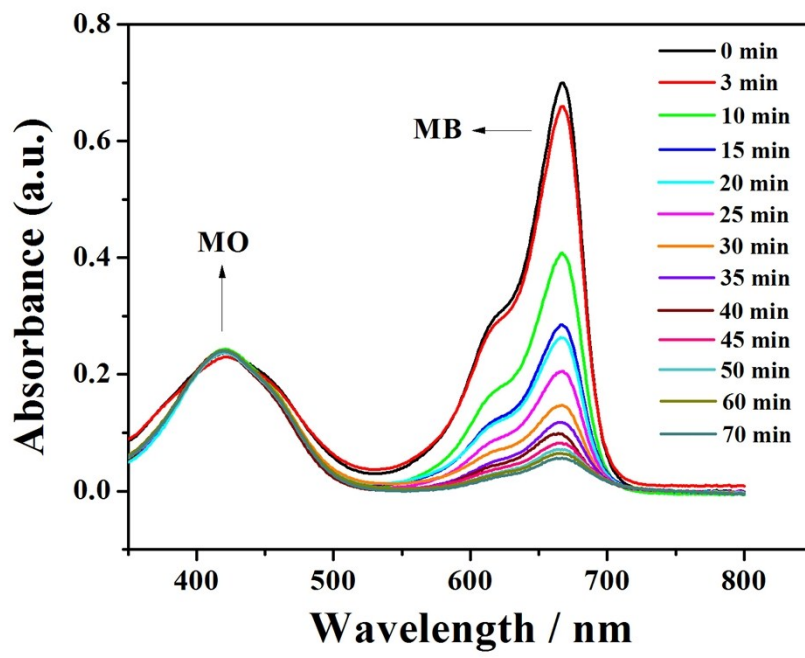


Fig. S8 UV/Vis spectra of DMA solution of mixed MB and MO with NENU-505.

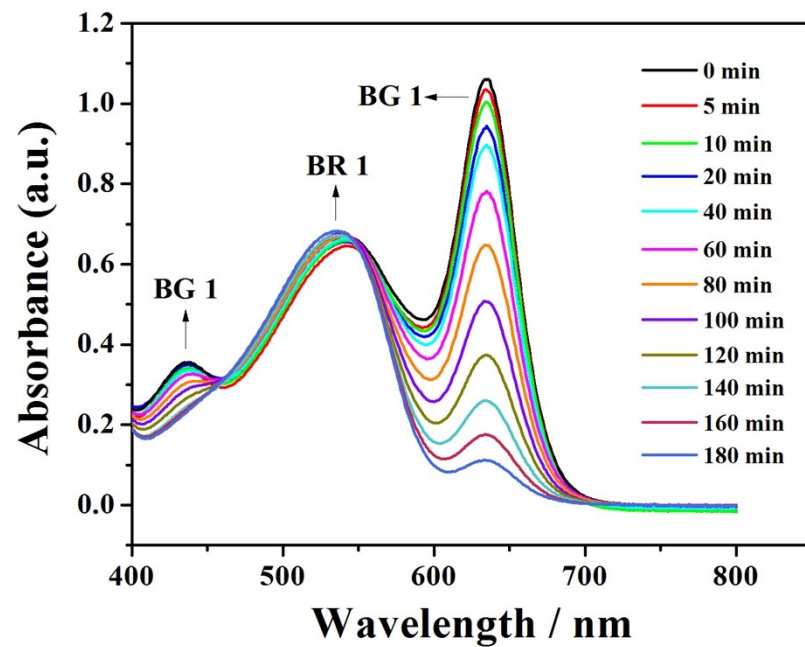


Fig. S9 UV/Vis spectra of DMA solution of mixed BG 1 and BR 1 with NENU-505.

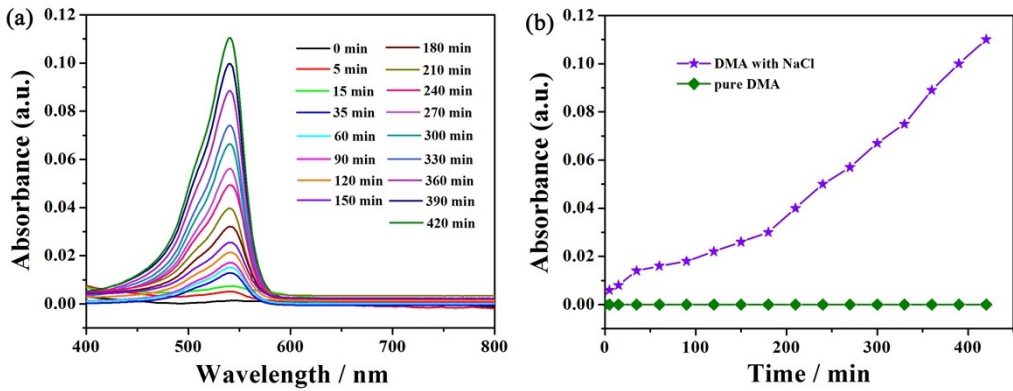


Fig. S10 (a) The BR 2 released from **BR 2@NENU-505** in a saturated solution of NaCl in DMA monitored by UV absorption. (b) The release-rate comparison of BR 2 from **BR 2@NENU-505** in a saturated solution of NaCl in DMA (purple) and pure DMA (dark green).

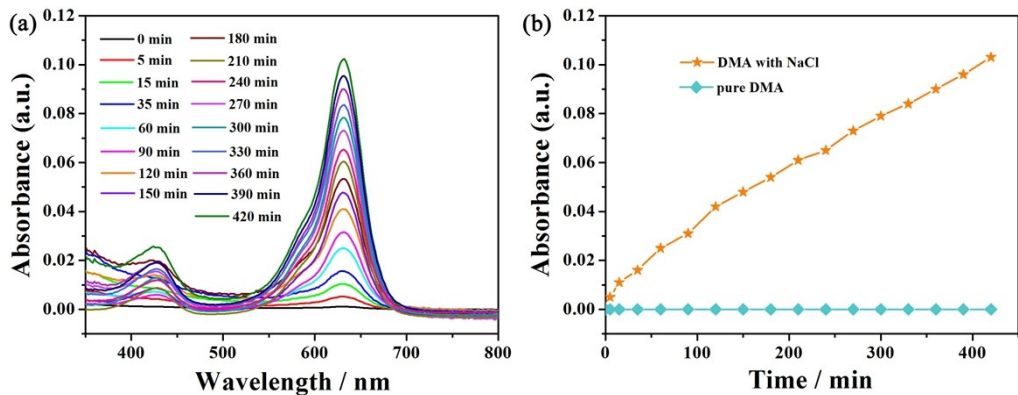


Fig. S11 (a) The BG 1 released from **BG 1@NENU-505** in a saturated solution of NaCl in DMA monitored by UV absorption. (b) The release-rate comparison of BG 1 from **BG 1@NENU-505** in a saturated solution of NaCl in DMA (orange) and pure DMA (pale green).

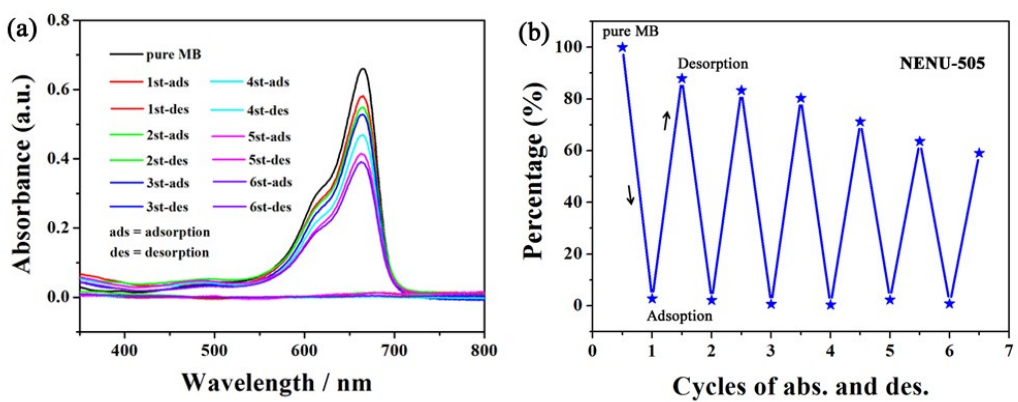


Fig. S12 (a) UV-vis spectra of MB solution in DMA after adsorption experiments with **NENU-505**, as well as the MB released (desorption) from **MB@NENU-505** using a saturated solution of NaCl in DMA. (b) The adsorption and desorption efficiency of **NENU-505** toward MB after six cycles.

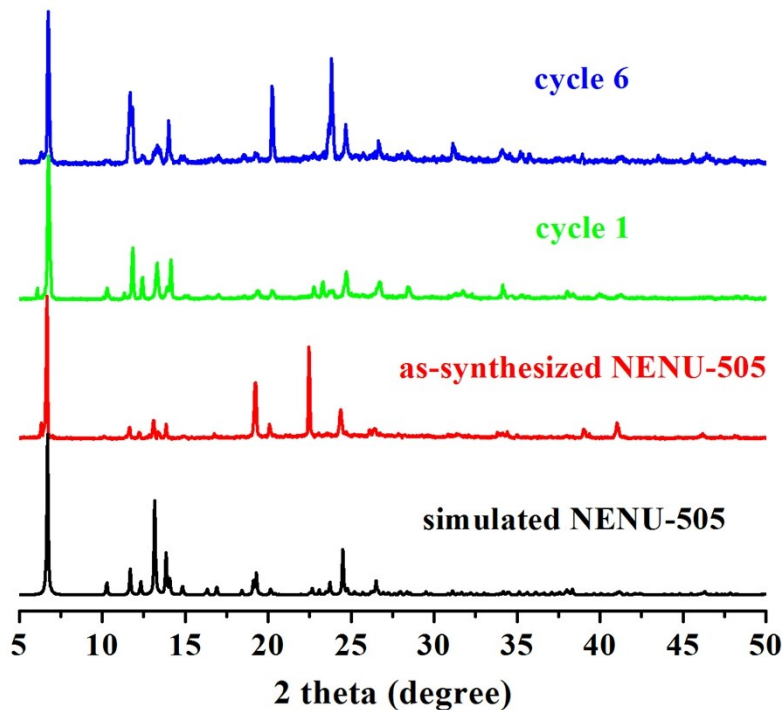


Fig. S13 XRPD patterns of **NENU-505** toward MB after adsorption–desorption cycle 1 and cycle 6.

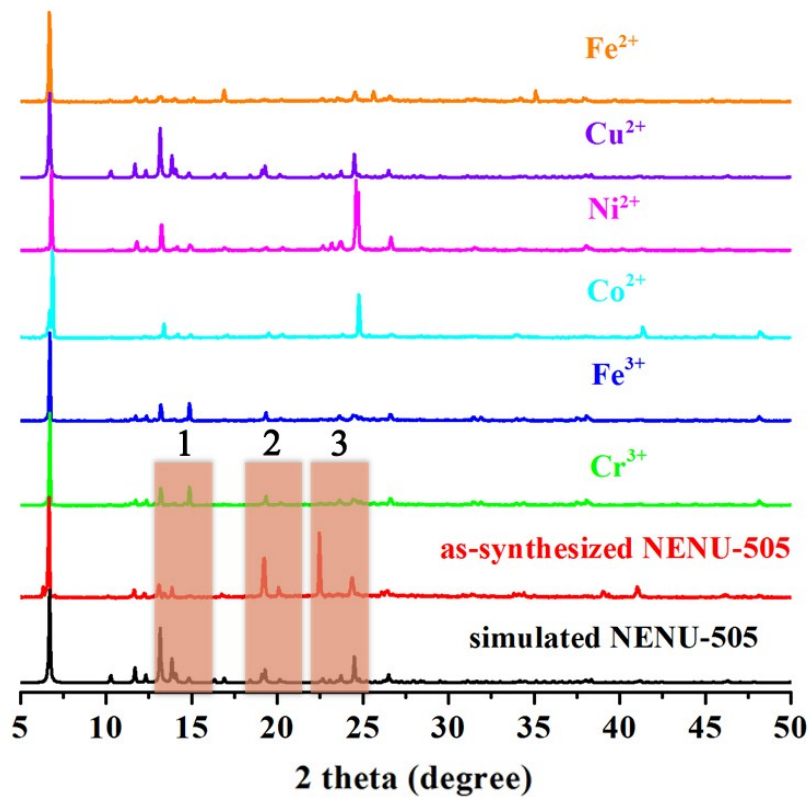


Fig. S14 XRPD patterns of NENU-505 immersed in different metal ions.

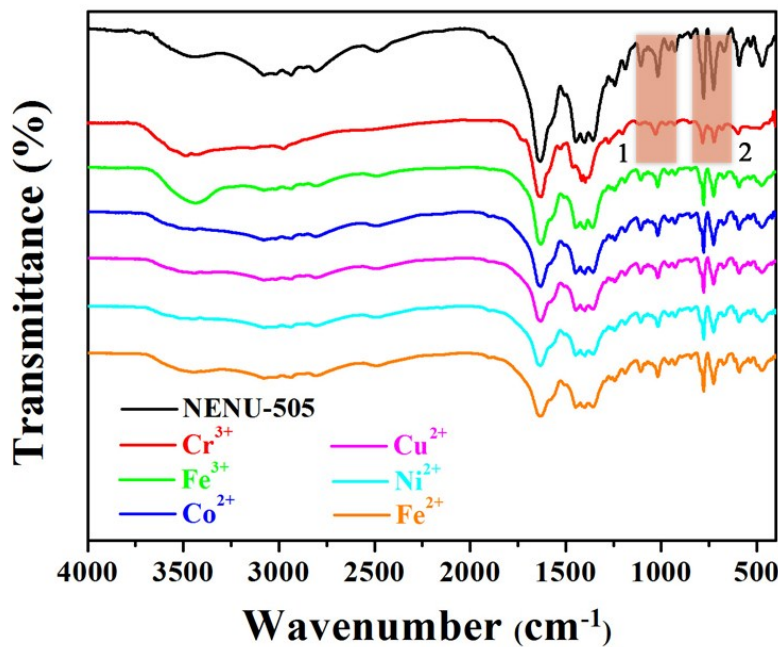


Fig. S15 IR spectra of NENU-505 immersed in different metal ions.

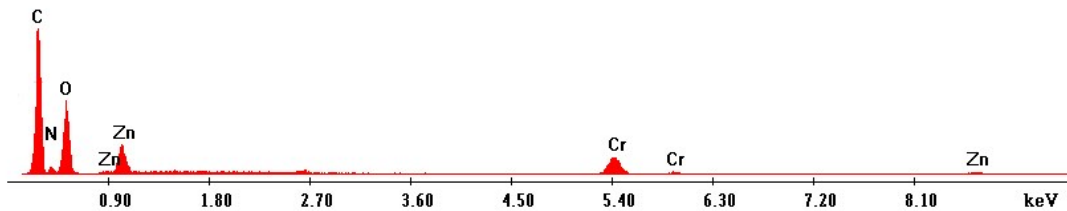


Fig. S16 EDS analysis of Cr^{3+} @NENU-505.

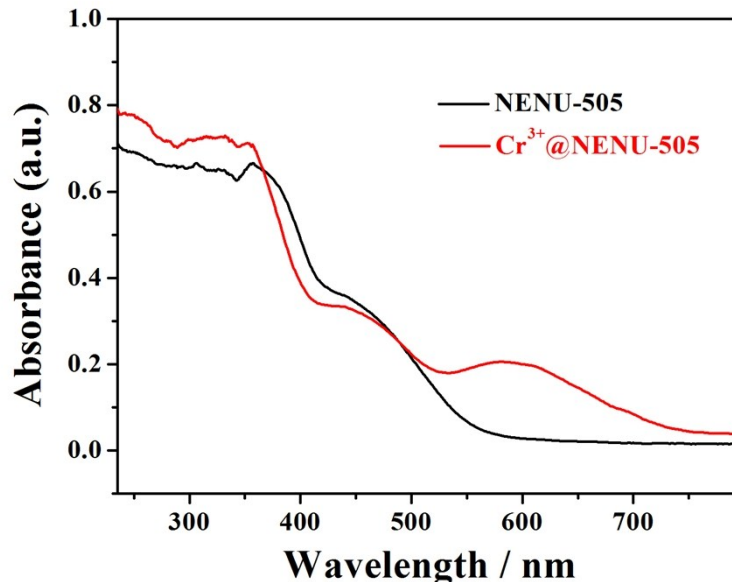


Fig. S17 UV/Vis spectra of solid NENU-505 and Cr^{3+} @NENU-505.

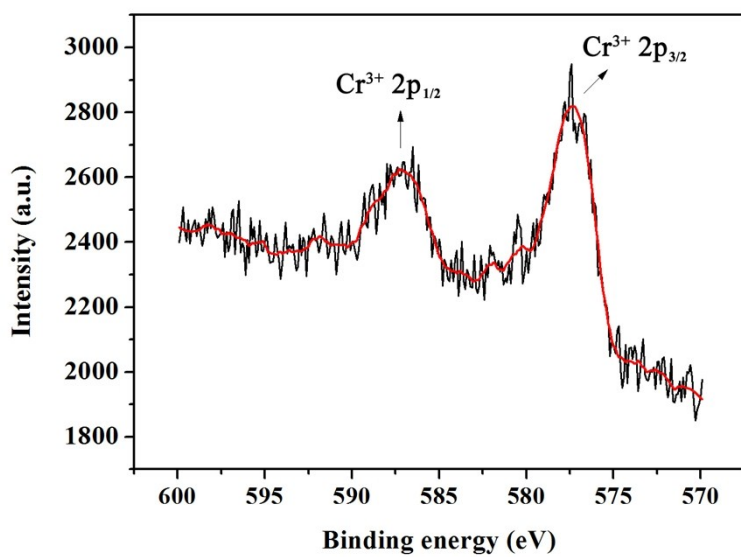


Fig. S18 XPS spectrum of Cr^{3+} for Cr^{3+} @NENU-505.

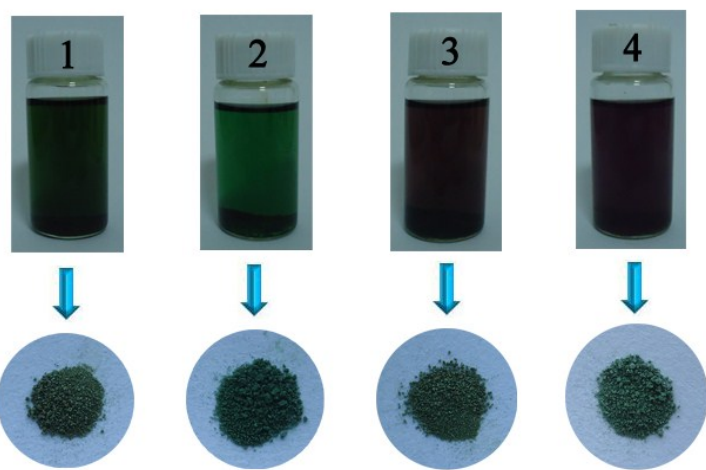


Fig. S19 The photographs of **NENU-505** in 10 mL DMA solutions containing three equal concentration of each metal ion (1: Fe^{2+} , Cu^{2+} and Cr^{3+} ; 2: Cu^{2+} , Ni^{2+} and Cr^{3+} ; 3: Cu^{2+} , Co^{2+} and Cr^{3+} ; 4: Ni^{2+} , Co^{2+} and Cr^{3+} , 0.01 M).

Notes and References

- 1 J.-D. Xiao, L.-G. Qiu, X. Jiang, Y.-J. Zhu, S. Ye and X. Jiang, *Carbon*, 2013, **59**, 372.
- 2 F.-Y. Yi, W. Zhu, S. Dang, J.-P. Li, D. Wu, Y.-h. Li and Z.-M. Sun, *Chem. Commun.*, 2015, **51**, 3336.
- 3 A.-X. Yan, S. Yao, Y.-G. Li, Z.-M. Zhang, Y. Lu, W.-L. Chen and E.-B. Wang, *Chem. Eur. J.*, 2014, **20**, 6927.
- 4 F.-Y. Yi, J.-P. Li, D. Wu and Z.-M. Sun, *Chem. Eur. J.*, 2015, **21**, 11475.
- 5 The national standard of the People's Republic of China: wooden granular activated carbon for water purification. GB/T13803.2-1999.
- 6 Y. Zhu, Y.-M. Wang, S.-Y. Zhao, P. Liu, C. Wei, Y.-L. Wu, C.-K. Xia and J.-M. Xie, *Inorg. Chem.*, 2014, **53**, 7692.
- 7 L. Li, X. L. Liu, H. Y. Geng, B. Hu, G. W. Song and Z. S. Xu, *J. Mater. Chem. A*, 2013, **1**, 10292.
- 8 M. Du, X. Wang, M. Chen, C.-P. Li, J.-Y. Tian, Z.-W. Wang and C.-S. Liu, *Chem. Eur. J.*, 2015, **21**, 9713.
- 9 C.-Y. Sun, X.-L. Wang, C. Qin, J.-L. Jin, Z.-M. Su, P. Huang and K.-Z. Shao, *Chem. Eur. J.*, 2013, **19**, 3639.